IEEE Access
Multidisciplinary | Rapid Review | Open Access Journal

Received July 27, 2021, accepted August 7, 2021, date of publication August 24, 2021, date of current version September 3, 2021.

Digital Object Identifier 10.1109/ACCESS.2021.3107095

Global Characterization of Linear Statistically Thinned Antenna Arrays

GIOVANNI BUONANNO[1] **AND RAFFAELE SOLIMENE**[1,2,3] **(Senior Member, IEEE)**

[1]Department of Engineering, University of Campania Luigi Vanvitelli, 81031 Aversa, Italy
[2]Consorzio Nazionale Interuniversitario per le Telecomunicazioni, 43124 Parma, Italy
[3]Department of Electrical Engineering, Indian Institute of Technology Madras, Chennai 600036, India

Corresponding author: Giovanni Buonanno (giovanni.buonanno@unicampania.it)

ABSTRACT In this paper we consider the characterisation of linear statistically thinned arrays. Their side-lobe level is often given in terms of the angle independent array factor variance, which does not capture the actual statistical fluctuations of the power pattern around its average, or by some analytical formulas which overcome this limitation by estimating the probability distribution of the peak side-lobe level. Here, the aim is to refine existing theory in order to obtain a more precise estimation of the statistical features of thinned arrays. For the general asymmetric case, we exploit an analytical expression of the variance of the power pattern. This measures the dispersion of the power pattern around its average and in conjunction with the Chebyshev's inequality allows to find a lower bound, for each fixed angle, of the power pattern probability distribution. For symmetric thinned arrays, the power pattern probability distribution is precisely obtained without resorting to some strong assumptions which are usually employed to get tractable expressions. Also, this result, along with the up-crossing method, allows to obtain a theoretical and new expression for the peak side-lobe level probability distribution as well as for the deviation between the thinned array factor and the reference one. The theoretical findings are checked through a Monte Carlo numerical analysis. The numerical results show that the theoretical predictions work very well and are more accurate than previous literature estimations. Finally, since the symmetric thinned arrays actually exploit half the available degrees of freedom, a numerical comparison is run with the asymmetric ones. The comparison shows that asymmetric and symmetric statistically thinned arrays exhibit similar performances.

INDEX TERMS Density-tapered arrays, nonuniformly-spaced arrays, random arrays, side-lobe level characterisation, standardised error characterisation, thinned arrays.

I. INTRODUCTION

Nonuniformly-spaced arrays consist of elements arranged at a non-constant separation spacing [1]. They are of interest since fewer elements than uniformly-spaced arrays can be employed and, in principle, the array factor shaping can be achieved without the amplitude-tapering [2], [3].

Different strategies, such as heuristic, deterministic, probabilistic (the ones of interest herein) and optimisation based approaches, have been proposed for obtaining a non-uniform arrangement.

The paper by Unz [4] is most likely the first one that deals with non-uniformly spaced arrays and addresses their study using matrix techniques.

The associate editor coordinating the review of this manuscript and approving it for publication was Chan Hwang See.

The paper by Willey [5] and the contribution by Doyle [1] can be considered the pioneering and seminal results towards the development of the deterministic density-tapering. Basically, these approaches are founded in some procedures by which the spatial density of a nonuniformly-spaced array is determined according to the amplitude tapering of a reference array. In this framework, the contribution by Willey is rather heuristic but provides an estimation of the peak side-lobe level (*PSLL*) in terms of the number of elements and their average separation. Note that this estimation is the same as reported by Andreasen [6]. Doyle theory is more rigorous. Indeed, it shows how to non-uniformly deploy the elements so as to minimise a weighted square error metric. This metric tends to promote good pattern matching (between the reference and the non-uniform one) especially around the main beam. This justifies the increasing of side-lobes far from

the main beam, which is commonly experienced by space tapering procedures.

The contribution by Harrington [7] mainly concerns the reduction of the side-lobe level (*SLL*) by introducing small perturbations of the initial uniform positions.

The contribution by Bucci *et al.* [2] presents a modified Doyle approach for the case of linear arrays, whereas [8] focuses on the application of the Doyle method to circularly symmetric arrays.

Another noteworthy methodology is that of Ishimaru *et al.* [9]–[11], in which the analysis/synthesis of nonuniformly-spaced arrays is carried out by transforming the array factor using the Poisson summation formula and hence introducing the so-called source number and source position functions. This way, the array factor is recast as a sum of an infinite number of radiation patterns due to continuous sources. However, this methodology does not allow for a simple generalisation of the synthesis process since, in order to obtain analytically tractable relations, it is necessary to impose some constraints on the source number and source position functions.

As to the statistically designed density-tapered arrays (statistically thinned arrays), the contributions by Skolnik *et al.* [12] and by Lo [13] are the most theoretically significant for research in this field. In particular, Skolnik *et al.* [12] focus on statistically thinned arrays which are obtained by randomly removing elements from the reference filled array according to a probabilistic law dictated by the amplitude tapering of the reference one. However, their theory covers up to the estimation of the variance of the array factor, which is considered as the average *SLL*. Lo [13] also considered the case of statistically thinned arrays. In particular, he adopted the same methodology as he developed for the so-called totally random arrays [14], by considering highly thinned cases. The estimation of the *PSLL* is correctly cast as the statistical characterisation of the supremum of the array factor magnitude in the side-lobe region but the sampling method is adopted, which is theoretically questionable and does not necessarily return accurate results. Also, the array factor is assumed stationary.

Finally, there is a large body of research that casts the synthesis of arrays, and particularly of the thinned ones, as an optimization problem and many different algorithms have been presented in the literature. [15].

In this paper we focus only on statistically thinned arrays. Although they have been around for a long time, they are still of interest because of their simplicity and since there are several scenarios, such as satellite communications, radio-astronomy, ground-based high-frequency radars, where achieving high-resolution is required by keeping, at the same time, the system as cheap and light as possible [16]. Moreover, recently it has been suggested that statistically thinned arrays can be conveniently used in the framework of smart antennas and in particular for adaptive beam-forming in order to cancel the interference coming from outside the main beam [17], [18].

Statistically thinned arrays are often characterised in terms of the average *SLL*, which is the variance of the array factor [12]. This simple characterisation however misses to capture the actual statistical fluctuations of the power pattern around its average. To overcome this limitation some *PSLL* estimations have been presented in the literature. Here, we mention the one reported in [6] and the Brookner one [15], [17], which here will be used as benchmark. The latter, in particular, returns an estimation of the probability distribution of the *PSLL* and basically is adapted from the Lo results [13].

Here, the aim is to provide a more complete theoretical framework for characterising the stochastic thinned array factor with respect to [12], estimating the dispersion (with respect to the reference array) of both the array factor and the power pattern as well as the *PSLL* probability distribution. In particular, for the case of symmetric thinned arrays, we refine the Lo approach [13] by avoiding some strong assumptions concerning the statistical nature of the array factor.

The content conveyed in this paper is the following. In Section II, basics on linear statistically thinned arrays are briefly recalled under the general asymmetric framework. The aim is to establish the background and the notation. Moreover, in this section, using the Chebyshev's inequality, we find a lower bound, for each angle, for the probability that the power pattern is inside a given interval. This result allows to have a better characterisation, with respect to the simple array factor variance, of the power pattern fluctuations and seems to have been overlooked in the pertinent literature. In Section III, symmetric thinned arrays are presented along with their exact probability distribution. This allows to compute the probability (no longer only a lower bound) that the array factor is within a given interval, for each observation angle. Afterwards, in Section IV, the probability distributions of the *PSLL* and of the supremum of the *standardised error* magnitude (between the thinned array factor and the reference one) are derived for the symmetric case, whereas in Section V a Monte Carlo numerical analysis is used to check the theoretical findings. The numerical analysis shows that these findings work very well and, above all, allows for a more accurate characterisation of the *PSLL* than the literature formulas mentioned above. In this Section, we also numerically address the comparison between the symmetric and the asymmetric thinned arrays. This is done in order to appreciate how the reduction by half of the available degrees of freedom (due to the symmetric arrangement) impacts on the array statistical features. Finally, conclusions and future developments end the paper. The paper also includes a short appendix that reports the expressions of some functions used and not described in the main text.

We end this section by remarking that here the focus is only on the array factor. Hence, isotropic radiators are considered and mutual coupling neglected. These, however, are the starting point assumptions commonly used in the

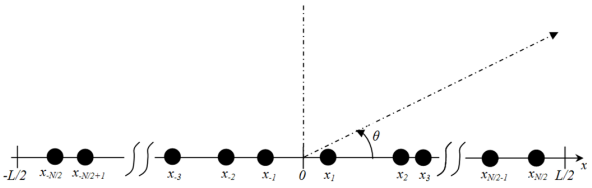

FIGURE 1. Geometry of a generic asymmetric array.

literature [15], [24], [25]. Also, for thinned arrays, mutual coupling can be considered less severe [15], [18].

II. BASICS ON STATISTICALLY THINNED ARRAYS

Consider a linear array of N isotropic radiators deployed along the x axis within the segment $[-L/2, L/2]$ (see Fig. 1). Denote its array factor as

$$F_{REF}(u) = \sum_{n=-N/2}^{N/2} A_n e^{j2\pi x_n u} \tag{1}$$

in which, for simplicity, N is assumed even and there is no element with $n = 0$. Moreover,

- $\{A_n\}_{n=-N/2}^{N/2}$ are the excitation coefficients (amplitude taper) determined according to the desired array factor shape;
- $u = (\cos\theta - \cos\theta_o)$, with θ and θ_o being the observation and the steering angles measured from the axis of the array, respectively;
- $x_n \in [-L/2, L/2]$ is the (deterministic) position of the n-th radiator, measured in wavelength. The $\{x_n\}_{n=-N/2}^{N/2}$ do not necessarily need to be uniform across the array aperture. Here, however, we limit to consider the case whereby the spacing between adjacent radiators is 0.5 (*i.e.*, $\lambda/2$).

$F_{REF}(u)$ is the so-called reference filled array factor which must be approximated by the thinned array. If the thinning is statistically achieved, the corresponding array factor can be expressed as [12], [13]

$$F(u) = C \sum_{n=-N/2}^{N/2} F_n e^{j2\pi x_n u} \tag{2}$$

in which

- $\{F_n\}_{n=-N/2}^{N/2}$ are independent Bernoulli random variables;
- C is a suitable real constant.

In particular, $\mathcal{P}\{F_n = 1\} = p_n$, $\mathcal{P}\{F_n = 0\} = 1 - p_n$, with $0 \le p_n = \alpha A_n / \max\{A_n\} \le 1$, $C = \max\{A_n\}/\alpha$ and $0 < \alpha \le 1$ is the *thinning factor*; when $\alpha = 1$ it is said that a *natural thinning* is achieved.

Since the excitation coefficients in (2) are random variables, the array factor is a stochastic process. Its mean and variance and the average power pattern are easily found to be [12]

$$\overline{F(u)} = F_{REF}(u) = \mu(u) \tag{3}$$

$$\begin{aligned}\sigma^2 &= \overline{|F(u)|^2} - |F_{REF}(u)|^2 = \overline{P(u)} - |F_{REF}(u)|^2 \\ &= \sum_{n=-N/2}^{N/2} (A_n/\alpha)(\max\{A_n\} - \alpha A_n)\end{aligned} \tag{4}$$

and

$$\overline{P(u)} = |F_{REF}(u)|^2 + \sigma^2 \tag{5}$$

in which $\overline{(\cdot)}$ denotes the statistical expectation and $P(u)$ is the power pattern. It is noted that, thanks to the choice of C, $\overline{F(u)}$ coincides with the (desired) reference array factor $F_{REF}(u)$.

The variance σ^2 is often employed as a *rough* estimation of the side-lobe level. However, this does not precisely capture the *fluctuations* that the power pattern exhibits around its average. More accuracy can be gained by finding the cumulative distribution function (*cdf*) of $P(u)$, that is

$$P_r(P(u) < \xi^2) = P_r(|F(u)| < \xi) \tag{6}$$

When N is large and $A_{-n} = A_n$, the Lyapunov's Central Limit Theorem (CLT) can be invoked and the real ($F_{\mathcal{R}}(u)$) and the imaginary ($F_{\mathcal{I}}(u)$) parts of $F(u)$ are jointly normal [14] and uncorrelated. Therefore, (6) is a generalised non-central chi-square distribution with two degrees of freedom, which, however, does not admit a closed form expression [14]. Moreover, it can be easily shown that $\mu_{\mathcal{R}}(u) = \mu(u)$, $\sigma_{\mathcal{R}}(u)$ and $\sigma_{\mathcal{I}}(u)$, *i.e.*, the mean of the real part, the standard deviations of the real and imaginary parts of the array factor (see the appendix for their expressions) are periodic functions. Therefore, the array factor stationary assumption [14], [19], which greatly simplifies the matter and allows to find an approximation of (6), cannot be rigorously employed. Nonetheless, it is at least possible to obtain the variance of the power pattern that measures the dispersion of the latter around its average. In particular, by taking into account the expressions of the higher order moments of a Gaussian random variable, we obtain

$$\begin{aligned}\sigma_P^2(u) &= \overline{P^2(u)} - \overline{P(u)}^2 \\ &= \overline{F_{\mathcal{R}}^4(u)} + \overline{F_{\mathcal{I}}^4(u)} - \overline{F_{\mathcal{R}}^2(u)}^2 - \overline{F_{\mathcal{I}}^2(u)}^2 \\ &= 4F_{REF}^2(u)\sigma_{\mathcal{R}}^2(u) + 2\sigma_{\mathcal{R}}^4(u) + 2\sigma_{\mathcal{I}}^4(u)\end{aligned} \tag{7}$$

Hence, (7) can be employed in conjunction with the Chebyshev's inequality

$$P_r\left\{|P(u) - \overline{P(u)}| < k\,\sigma_P(u)\right\} \ge 1 - \frac{1}{k^2} \tag{8}$$

with $k > 1$, to find a lower bound for the probability that the power pattern, at u, is inside the interval $[\overline{P(u)} - k\,\sigma_P(u), \overline{P(u)} + k\,\sigma_P(u)]$.

For thinned arrays, the number of elements that populate the array is the random variable $N_A = \sum_{n=-N/2}^{N/2} F_n$, with mean $\bar{N}_A = (\alpha/\max\{A_n\})\mu(0)$ and variance $\sigma_{N_A}^2 = (\alpha/\max\{A_n\})^2\sigma^2$ and, because of the CLT, normal probability distribution $N_A \sim \mathcal{N}(\bar{N}_A, \sigma_{N_A}^2)$.

Furthermore, since the spacing between adjacent radiators is 0.5, then the directivity (and hence the gain since we are considering ideal radiators) coincides with N_A.

III. SYMMETRIC THINNED ARRAYS

A more accurate statistical characterisation of thinned arrays can be achieved if the array is assumed to be symmetric [20]. Basically, under the same framework as above, it is further assumed that only half of the reference array is thinned, then for each elemental radiator that survived the thinning procedure, another one is symmetrically (with respect to the array centre) deployed over the other half part. The corresponding thinned array factor is then

$$F_s(u) = 2C \sum_{n=1}^{N/2} F_n \cos(2\pi x_n u) \tag{9}$$

The CLT again yields $F_s(u) \sim \mathcal{N}[\mu_s(u), \sigma_s^2(u)]$, with

$$\mu_s(u) = F_{REF}(u) \tag{10}$$

and

$$\sigma_s^2(u) = 4 \sum_{n=1}^{N/2} (\max\{A_n\} A_n/\alpha - A_n^2) \cos^2(2\pi x_n u) \tag{11}$$

At this juncture, an analogous of (8) can be obtained as well. However, in this case it is possible to determine the distribution of the power-pattern (or of the array factor magnitude) in a very simple way, without resorting to any approximation [20]. Indeed, in this case it is easy to verify that

$$\begin{aligned} P_r\left\{P_s(u) \le \xi^2\right\} &= P_r\left\{|F_s(u)| \le \xi\right\} \\ &= Q\left(\frac{-\xi - \mu_s(u)}{\sigma_s(u)}\right) - Q\left(\frac{\xi - \mu_s(u)}{\sigma_s(u)}\right) \end{aligned} \tag{12}$$

with $P_s(u)$ being the power pattern for the symmetric case and $Q(\cdot)$ can be expressed in terms of the error function. In particular, also the mean and the variance of the array factor magnitude can be easily evaluated in closed-form [20].

It is remarked that (12) can be rewritten so that the arguments of the Q-functions are positive and hence the Q-functions can be approximated by the polynomial expression reported in [26] and [27], thus avoiding the use of tabulated functions.

Moreover, instead of a lower bound as in (8), here the η-percent level curve $r_\eta(u)$ can be precisely found as [20]

$$\begin{aligned} &P_r\left\{|F_s(u)| \le r_\eta(u)\right\} \\ &\quad = Q\left(\frac{-r_\eta(u) - \mu_s(u)}{\sigma_s(u)}\right) - Q\left(\frac{r_\eta(u) - \mu_s(u)}{\sigma_s(u)}\right) = \eta\% \end{aligned} \tag{13}$$

Alternatively, one may be interested in how much the array factor deviates from the reference one. In this circumstance, say $LB(u) = \mu_s(u) - \xi\,\sigma_s(u)$ and $UB(u) = \mu_s(u) + \xi\,\sigma_s(u)$ the lower and upper *barriers* within which $F_s(u)$ should be confined, then (13) particularizes as [29]

$$P_r\left\{LB(u) \le F_s(u) \le UB(u)\right\} = Q(-\xi) - Q(\xi) \tag{14}$$

Also for symmetric thinned arrays the actual number of antenna elements is a random variable now given as $N_{As} = 2\sum_{n=1}^{N/2} F_n$, with mean $\bar{N}_{As} = (\alpha/\max\{A_n\})\mu(0)$ and variance $\sigma^2_{N_{As}} = (\alpha/\max\{A_n\})^2\sigma_s^2(0)$. As for the previous case, the directivity coincides with N_{As}.

IV. GLOBAL CHARACTERISATION

In the previous sections, we have shown that it is possible to estimate the fluctuations of the power pattern through (8), for the general asymmetric thinned arrays, and more precisely through (13) or (14), for symmetric arrays. However, those estimations are indeed punctual since the array factor is characterised for each fixed u but not simultaneously over a given internal of the angular variable. In order to estimate the *PSLL*, as remarked in [14], one has to find the probability distribution of the supremum of the array factor magnitude in the whole side-lobe region. Analogously, previous formulas can only allow to estimate (statistically) the deviation of the array factor from the reference one for each given u, whereas information relating to the entire observation range cannot be determined.

To this end, in this section, we adapt to the present case the methodologies introduced in [20] and [28]–[33], in which random arrays were considered.

A. PSLL CHARACTERISATION

According to Skolnik *et al.*[12], the average relative side-lobe level ($\overline{SLL}$), when the excitation coefficients are real, can be estimated as the ratio between the variance of the array factor and the maximum value of the power-pattern mean, that is

$$\overline{SLL} = \frac{\sigma^2}{\overline{P(0)}} \tag{15}$$

For symmetric thinned arrays, the variance of the array factor is a function of u and so is the average relative side-lobe level. In this regard, a more conservative definition, which is analogous to (15), can be given as

$$\overline{SLL} = \frac{\sigma_s^2(0)}{\overline{P_s(0)}} \tag{16}$$

with $\sigma_s^2(0)$ being the maximum of the array factor variance.

However, often one is interested in determining the *PSLL*, which in turn requires finding the following distribution

$$\begin{aligned} P_r\left\{PSLL \le \xi\right\} &= P_r\left\{\left|\frac{F_s(u)}{F_s(0)}\right| \le \xi \ \forall\ u \in [u_1, u_2]\right\} \\ &= P_r\left\{\frac{P_s(u)}{P_s(0)} \le \xi^2 \ \forall\ u \in [u_1, u_2]\right\} \end{aligned} \tag{17}$$

It is seen that (17) only takes into account the positive values of the variable u, as for the case at hand, the array factor magnitude is an even function. Moreover, $u_1 > 0$ is assumed to be the positive first-null of $\mu_s(u)$ [13], [14], which basically represents the main-lobe half-width, and $u_2 > 0$ is the starting point of the first grating-lobe of $\mu_s(u)$ if the x_n are uniform, otherwise it is equal to 2.

Determining $P_r\{PSLL \leq \xi\}$ requires finding the probability distribution that a random process is below a given threshold over an interval of the variable u. This is a very difficult task that here is even more complex as compared to the case of equally-excited random arrays [14], [20], [28]. This is because, for statistically thinned arrays, $F_s(0) = 2C\sum_{n=1}^{N/2} F_n$ is a random variable as well, which is not independent on $F_s(u)$. Therefore, the distribution of $F_s(u)/F_s(0)$ is required. In order to avoid this difficulty, we instead consider a less complicated (though approximated) problem by assuming $F_s(0) \approx \mu_s(0)$. This assumption is justified by the fact that the coefficient of variation, $CV(u) = \sigma_s(u)/\mu_s(u) \gg CV(0)$ for $u > u_1$. This basically means that the dispersion of the array factor for $u = 0$ is less marked than in the side-lobe region. Note that this assumption is implicit in [13]. Accordingly, in order to estimate the *PSLL* distribution, we consider the simpler problem

$$P_r\left\{\widehat{PSLL} \leq \xi\right\} = P_r\left\{|\widehat{F}_s(u)| = \frac{|F_s(u)|}{|\mu_s(0)|} \leq \xi \ \forall\ u \in [u_1, u_2]\right\} \tag{18}$$

However, determining $P_r\{\widehat{PSLL} \leq \xi\}$ is still a difficult problem which has been approached by several approximate methods. Among them, the up-crossing method yielded in many cases better estimations [20], [28]–[33]. Therefore, it will be exploited herein. This method aims to estimate how many times the stochastic process $\widehat{F}_s(u)$ up-crosses (*i.e.*, crosses with a positive slope) a given level in the side-lobe region. Say ξ the level we are interested in and $\mathcal{N}_\xi$ the random variable that counts the times $|\widehat{F}_s(u)|$ up-crosses it, then $P_r\{\widehat{PSLL} \leq \xi\} = 1 - P_r\{\mathcal{N}_\xi \geq 1\}$. Hence, thanks to the Markov's inequality $P_r\{\mathcal{N}_\xi \geq 1\} \leq \overline{\mathcal{N}_\xi}$, a lower bound for $P_r\left\{\widehat{PSLL} \leq \xi\right\}$ can be achieved. However, a more precise result can be obtained. In fact, if it is assumed that the up-crossings occur according to a Poisson random point process [23], then [30], [31]

$$P_r\left\{\widehat{PSLL} \leq \xi\right\} \approx P_r\left\{|\widehat{F}_s(u_1)| \leq \xi\right\} e^{-\overline{\mathcal{N}_\xi}} \tag{19}$$

and (19) is the sought after estimation for the $\widehat{PSLL}$ distribution. However, we still need to compute $\overline{\mathcal{N}_\xi}$. To this end, following the seminal paper of Rice [34], and its development reported in [35] and [36], we obtain

$$\overline{\mathcal{N}_\xi} = \int_{u_1}^{u_2} du \int_0^\infty \gamma f_{|\widehat{F}_s||\widehat{F}_s|'}(\xi, \gamma; u) d\gamma \tag{20}$$

where $f_{|\widehat{F}_s||\widehat{F}_s|'}$ is the joint *pdf* of $|\widehat{F}_s(u)|$ and its first derivative in the side-lobe region. It is worth remarking that a completely analogous of (20) can be written for the case of asymmetric thinned arrays. However, in that case, an easy computation can be achieved only when $\widehat{F}(u)$ is assumed to be wide-sense stationary and by assuming the real and the imaginary parts of $\widehat{F}(u)$ and their derivatives being four uncorrelated and Gaussian processes [22]. These assumption do not hold true indeed. For the symmetric case, such assumptions are not required. In fact, since the array factor is a real process, the determination of the up-crossings of $|\widehat{F}_s(u)|$ is equivalent to the simultaneous study of the up-crossings of $\widehat{F}_s(u)$ and $\widetilde{F}_s(u) = -\widehat{F}_s(u)$. Since $\widehat{F}_s(u)$ and $\widehat{F}'_s(u) = d\widehat{F}_s(u)/du$ are jointly Gaussian (of course the same holds for $\widetilde{F}_s(u)$ and $\widetilde{F}'_s(u) = \widetilde{F}_s(u)/du$), then the expected number of the up-crossings of the level ξ is given as follows [35] (with u understood)

$$\begin{aligned}\overline{\mathcal{N}_\xi} = &\int_{u_1}^{u_2} \frac{\sigma_{F'}}{\sigma_s}\sqrt{1-\rho^2}\,\phi\left[\frac{\mu_s - \xi\,\mu_s(0)}{\sigma_s}\right] \\ &\times [\phi(\tau) + \tau\Phi(\tau)]\,du \\ &+ \int_{u_1}^{u_2} \frac{\sigma_{F'}}{\sigma_s}\sqrt{1-\rho^2}\,\phi\left[\frac{-\mu_s - \xi\,\mu_s(0)}{\sigma_s}\right] \\ &\times \left[\phi(\tau^*) + \tau^*\Phi(\tau^*)\right] du\end{aligned} \tag{21}$$

in which

$$\tau(u) = \frac{\sigma_s(u)\mu_{F'}(u) - \sigma_{F'}(u)\rho(u)[\mu_s(u) - \xi\,\mu_s(0)]}{\sigma_s(u)\sigma_{F'}(u)\sqrt{1-\rho^2(u)}} \tag{22}$$

$$\tau^*(u) = \frac{-\sigma_s(u)\mu_{F'}(u) + \sigma_{F'}(u)\rho(u)[\mu_s(u) + \xi\,\mu_s(0)]}{\sigma_s(u)\sigma_{F'}(u)\sqrt{1-\rho^2(u)}} \tag{23}$$

$\mu_{F'}(u)$ and $\sigma^2_{F'}(u)$ are the mean and the variance of $F'_s(u) = dF_s(u)/du$, respectively; $\rho(u)$ is the Bravais-Pearson correlation coefficient between $F_s(u)$ and $F'_s(u)$; $\Phi(x) = (2\pi^2)^{-1}\int_{-\infty}^{x} exp(-y^2/2)dy$ and $\phi(x) = d\Phi(x)/dx$ (see Appendix). As remarked above, (21) fully takes into account the non-stationarity of the array factor and the computation only requires a one-dimensional numerical integration (with respect to u). It is worth noting that for the asymmetric case, even under the approximate framework of [22], a two-dimensional numerical integration is required. Moreover, (21) is also an advance with respect to [20], in which a two-dimensional numerical integration is still required for the exact determination of $\overline{\mathcal{N}_\xi}$.

B. STANDARDISED ERROR

The same approach as used for the $\widehat{PSLL}$ characterisation can be followed in order to (statistically) quantify how much the thinned array factor deviates from the reference one. More in detail, as a measure of such a deviation we consider the *standardised error* $\epsilon(u) = [F_s(u) - \mu_s(u)]/\sigma_s(u)$. This choice is consistent with (14), which, however, provides the probability that $|\epsilon(u)| \leq \xi$ only for a fixed u. As remarked above, to globally characterise the deviation measure, we need it over a generic interval $[u_A, u_B]$ of the *full-scan range* $[-2, 2]$ [21]. This basically requires to rephrase (18) as

$$P_r\left\{\mathcal{S} = \max_{u\in[u_A,u_B]}\{|\epsilon(u)|\} \leq \xi\right\} \tag{24}$$

so that, by using once again the up-crossing method, it yields

$$P_r\{\mathcal{S} \leq \xi\} \approx P\{|\epsilon(u_A)| \leq \xi\}\, e^{-\overline{\mathcal{N}_\xi}} \tag{25}$$

in which the distribution of $|\epsilon(u_A)|$ is easily obtained from (12), and now

$$\overline{\mathcal{N}_\xi} = \int_{u_A}^{u_B} du \int_0^\infty \gamma f_{|\epsilon||\epsilon|'}(\xi, \gamma; u) d\gamma \tag{26}$$

with $f_{|\epsilon||\epsilon|'}$ being the joint *pdf* of $\epsilon(u)$ and its first derivative. Also for this problem, it is worth remarking that a completely analogous of (26) can be written for the case of asymmetric thinned arrays, but computation can be easily achieved only when $\epsilon_A(u) = [F(u) - \mu(u)]/\sigma(u)$ is assumed to be wide-sense stationary, which does not hold true. Instead, for symmetric thinned arrays, it is easily obtained and the mean of the up-crossings has a very simple and computationally convenient expression, that is

$$\overline{\mathcal{N}_\xi} = \sqrt{\frac{2}{\pi}}\,\phi(-\xi)\int_{u_A}^{u_B}\sigma_{\epsilon'}(u)\,du \tag{27}$$

in which $\sigma_{\epsilon'}(u)$ is the standard deviation of the derivative of $\epsilon(u)$ (see Appendix) and $\phi(x)$ is defined as in the previous section. Also, in deriving (27) it has been taken into account that $\epsilon(u)$ is a zero mean and unitary variance process and that the Bravais-Pearson correlation coefficient between $\epsilon(u)$ and its derivative is equal to zero (see Appendix).

V. NUMERICAL ASSESSMENT

In this section, some numerical examples are presented in order to validate the theoretical findings. In particular, we focus on the *PSLL* and the $\mathcal{S}$ distributions in (19) and (25), which globally characterise the array factor.

The experimental array factors are obtained via Monte Carlo simulations (2000 trials are used) by employing a sample step in the variable u of $1/(10L)$, which is 5 times smaller than the sampling step required by the bandwidth of the sample paths of the power pattern. Furthermore, the analysis is conducted only for $u \in [0, 1]$, as the array factor is an even and periodic function and therefore the information relative to the full-scan range, $[-2, 2]$, can be completely deduced starting from the interval $[0, 1]$. Therefore, in the following numerical analysis, u_1 is the positive first-null of $|\mu_s(u)|$, $u_2 = 1$ and $[u_A, u_B] \equiv [0, 1]$).

Two reference arrays are considered, with the excitation coefficients $\{A_n\}$ being samples of a Taylor current distribution [37] with $\bar{n} = 5$ and a side-lobe level equal to $-25dB$ (addressed as $F_{REF_1}(u)$) and $-35dB$ (addressed as $F_{REF_2}(u)$), respectively.

A. PSLL

In order to check the estimation of the *PSLL* distribution, we consider three cases: $N = 1000$, $N = 200$ and $N = 100$. It is worth remarking that for linear arrays the considered N may be excessive. However, examples of linear statistically thinned arrays with a very high initial number of elemental radiators can be found in the literature as in [15], where even $N = 5000$ was considered, and in [13] where N was set equal to 2×10^4. We would like to point out that the analysis here is carried out for linear arrays for the sake of simplicity. Indeed, it is applicable to any cut of the array factor of general planar/volumetric arrays, for which the number of elements can be actually high.

All the following figures in this section report the actual experimental distribution of the *PSLL* corresponding to $|F_s(u)/F_s(0)|$ (blue solid lines), the experimental distribution of the *PSLL* corresponding to the approximation $|F_s(u)/\mu_s(0)|$ (magenta solid lines) and the theoretical distribution (red dashed lines) returned by (19). Also, in order to compare our estimation with some previous literature results, two other curves are shown as well. In particular, the orange lines refer to the *PSLL* distribution resulting from the Andreasen formula (in *dB*), that is [6]

$$PSLL_{dB} = -10\log\left(\frac{N_{A_s}}{2}\right) - 10\log\left[\frac{1}{1-\frac{1}{2\,d_{AV}}}\right] \tag{28}$$

Note that N_{A_s} and d_{AV} (the average spacing between adjacent elements) are random variables and thence $PSLL_{dB}$ is also a random variable. Accordingly, the corresponding probability distribution is computed by using the 2000 trials as for (19). The black curves, instead, represent the Brookner estimation [15], [17]

$$P_r\{PSLL \le \xi\} = \left(1 - e^{-\overline{N}_{A_s}\xi^2}\right)^{\frac{N}{2}} \tag{29}$$

which basically is obtained from the Lo sampling method [13].

Looking at Figs. 2 and 3 it can be observed that the *PSLL* distribution weakly changes while passing from $F_{REF_1}(u)$ to $F_{REF_2}(u)$ and grows as the level of thinning increases. Indeed, as expected, as the degree of thinning increases, the curves move to the right. This, of course, is perfectly consistent with the remark reported many times in the literature that the *PSLL* mainly depends on the number of elements in the array. Also, it can be seen that the assumption $|F_s(u)/F_s(0)| \simeq |F_s(u)/\mu_s(0)|$ works very well. Finally, what is more, the theoretical *PSLL* distribution in (19) is practically overlapped to the actual one. This is true for both the considered cases and for all the levels of thinning. Hence, the derived theoretical *PSLL* distribution can be considered as an excellent tool to foresee the *PSLL* in relation to the level of thinning one may want to adopt. Note that this does not hold true for estimations given by (28) and (29).

Figs. 4 and 5 show the same comparison when $N = 200$ and $N = 100$, respectively. Here, only the case of $F_{REF_1}(u)$ is considered. As expected, the *PSLL* values increase as compared to the previous examples. However, what matters is that our estimation still shows an excellent agreement with the experimental distribution, which is by far much better than (28) and (29). It worth observing that the *PSLL* prediction through (29) improves when the degree of thinning increases. This could have been expected since, as remarked above, it is based on the results derived in [13], which works for highly thinned arrays. Nonetheless, our estimation is better even in these cases.

B. STANDARDISED ERROR

The probability distribution of the supremum of the standardised error magnitude, $\mathcal{S}$, introduced in (24) is checked in Figs. 6 and 7, which refer to the cases related to $F_{REF_1}(u)$

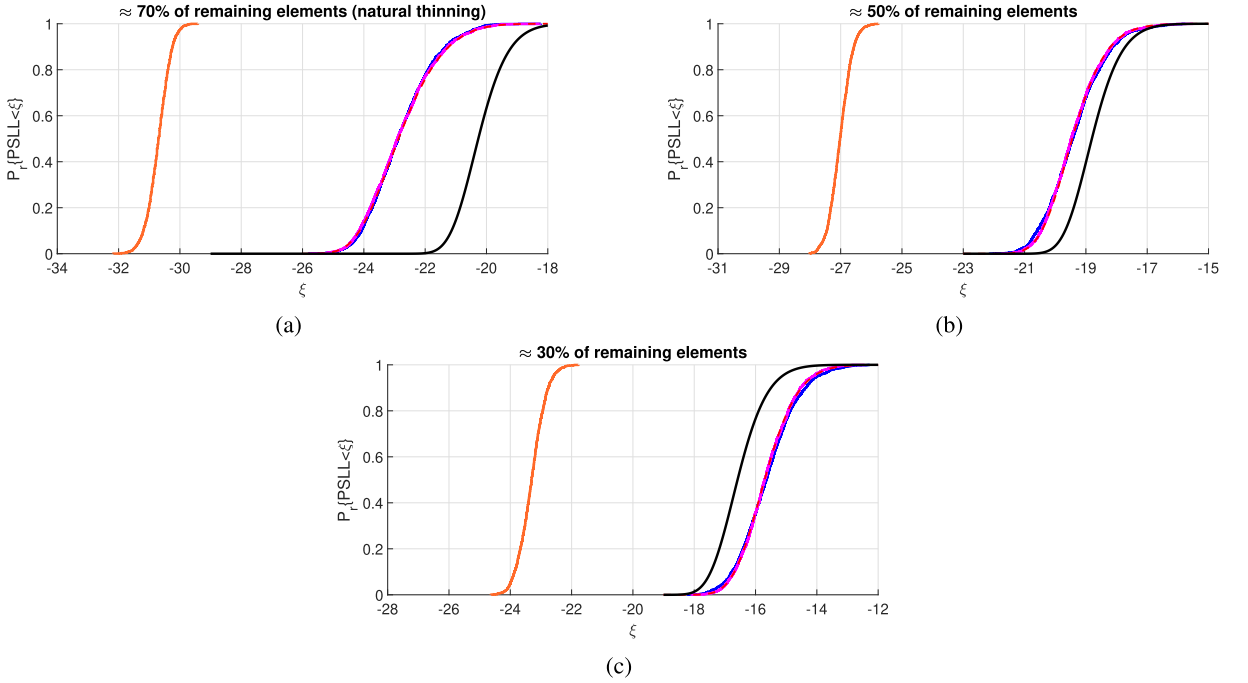

FIGURE 2. Probability distribution of *PSLL* for $F_{REF_1}(u)$, $N = 1000$ and different levels of thinning. Experimental distribution of the supremum of $|F_s(u)/F_s(0)|$ (blue solid lines), experimental distribution of the supremum of the approximation $|F_s(u)/\mu_s(0)|$ (magenta solid lines), our estimation returned by (19) (red dashed lines), estimation (28) (orange solid lines) and estimation (29) (black solid lines). The values of ξ are in *dB*.

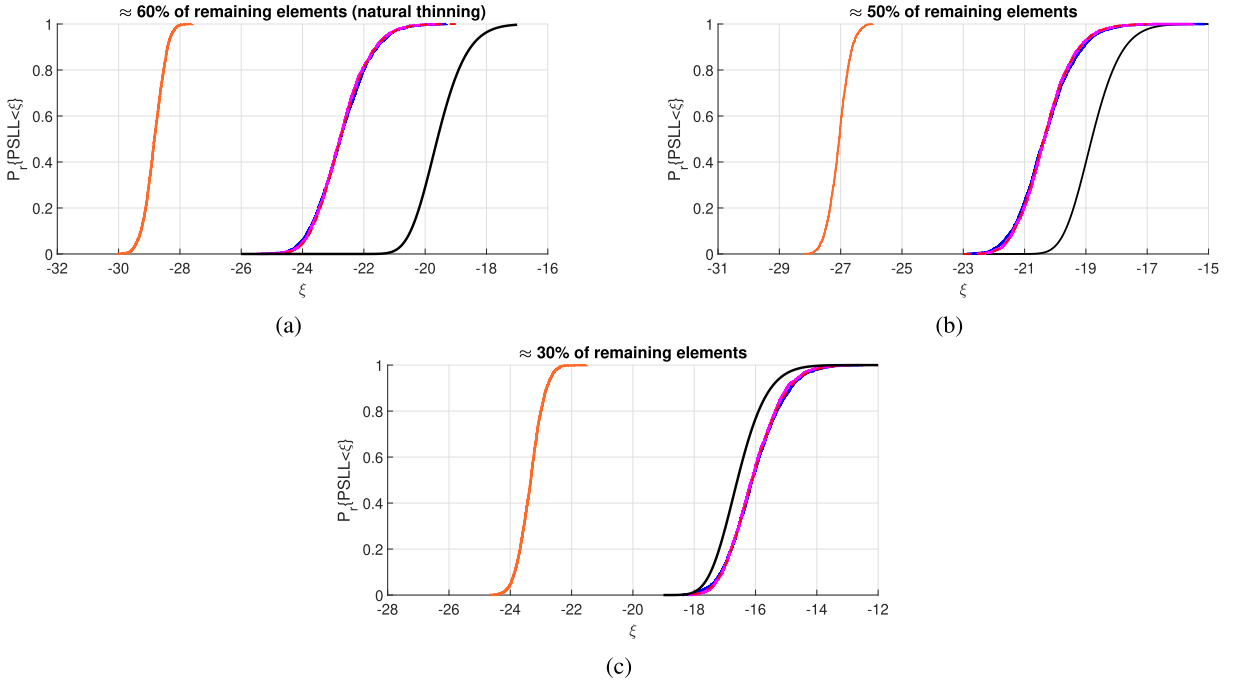

FIGURE 3. Probability distribution of *PSLL* for $F_{REF_2}(u)$, $N = 1000$ and different levels of thinning. Experimental distribution of the supremum of $|F_s(u)/F_s(0)|$ (blue solid lines), experimental distribution of the supremum of the approximation $|F_s(u)/\mu_s(0)|$ (magenta solid lines), our estimation returned by (19) (red dashed lines), estimation (28) (orange solid lines) and estimation (29) (black solid lines). The values of ξ are in *dB*.

and $F_{REF_2}(u)$, respectively. As can be seen, the experimental curves (in blue) and the theoretical prediction returned by (25) (in red), are very similar. Therefore, it can be concluded that (25) provides a very accurate estimation of the probability that a generic sample path of the array factor is *globally* between $\mu_s(u) - \xi\sigma_s(u)$ and $\mu_s(u) + \xi\sigma_s(u)$ (*i.e.*, *simultaneously* for each $u \in [0, 1]$). Hence, this error characterisation includes also the main beam region.

Some comments are in order. First, it is noted that the curves for different levels of thinning and for $F_{REF_1}(u)$ and

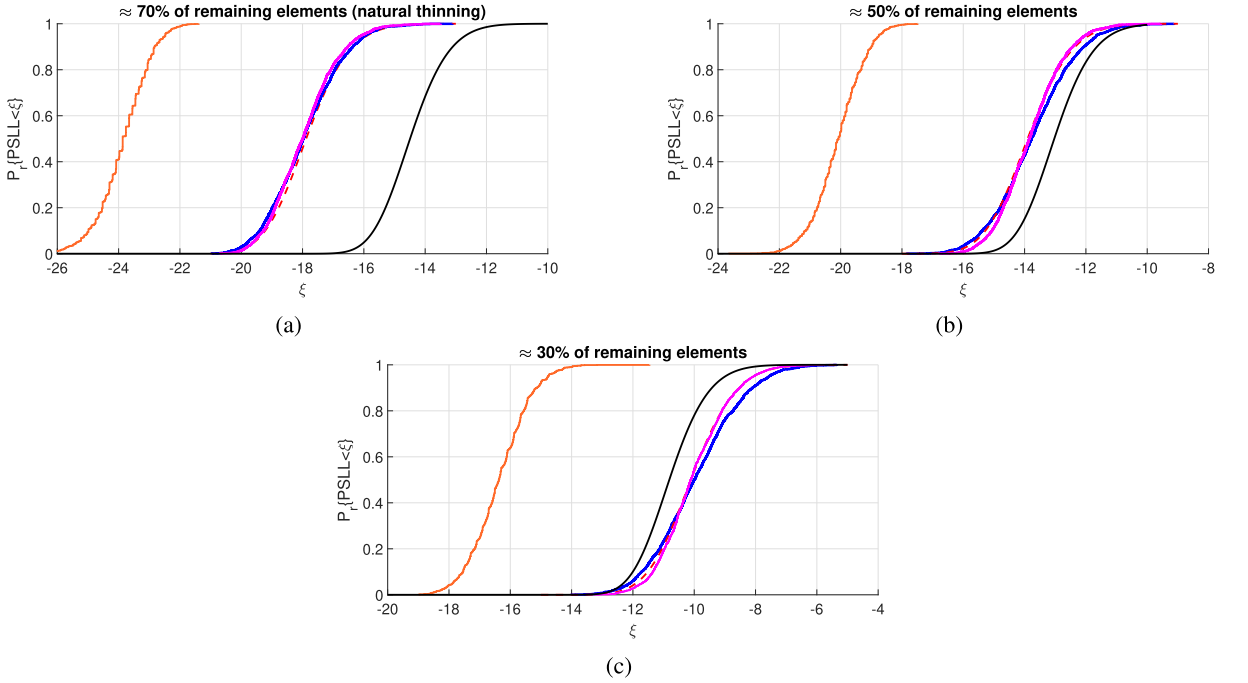

FIGURE 4. Probability distribution of *PSLL* for $F_{REF_1}(u)$, $N = 200$ and different levels of thinning. Experimental distribution of the supremum of $|F_s(u)/F_s(0)|$ (blue solid lines), experimental distribution of the supremum of the approximation $|F_s(u)/\mu_s(0)|$ (magenta solid lines), our estimation returned by (19) (red dashed lines), estimation (28) (orange solid lines) and estimation (29) (black solid lines). The values of ξ are in *dB*.

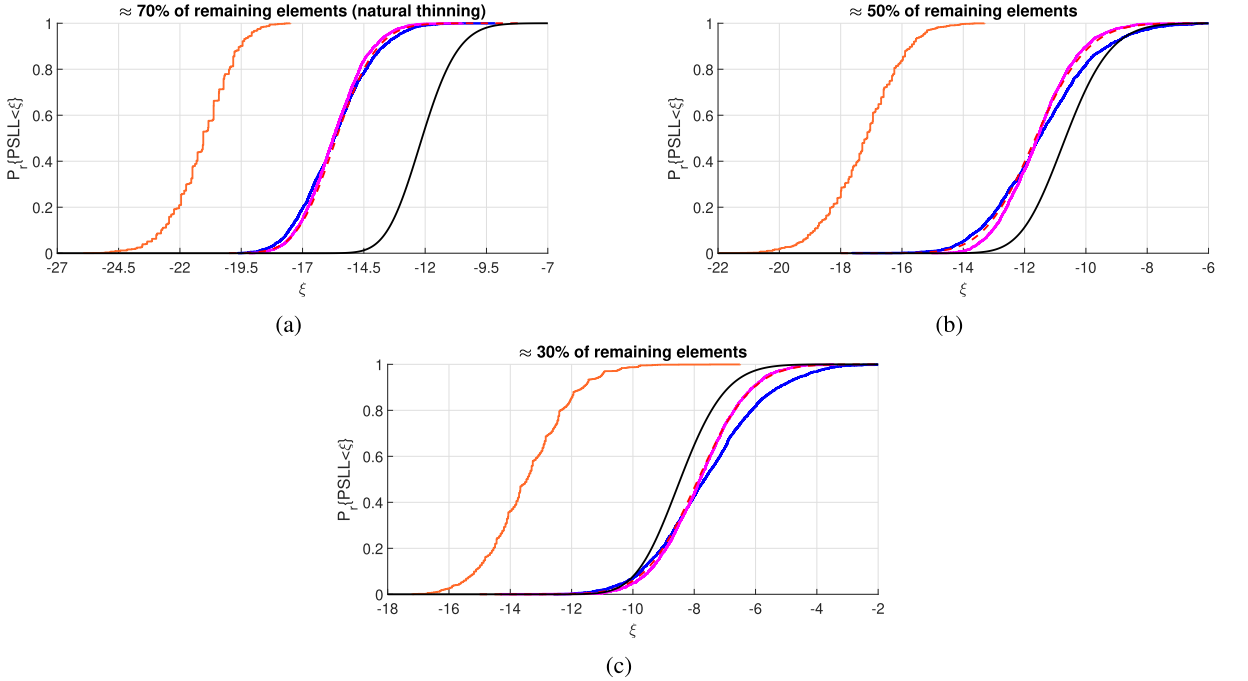

FIGURE 5. Probability distribution of *PSLL* for $F_{REF_1}(u)$, $N = 100$ and different levels of thinning. Experimental distribution of the supremum of $|F_s(u)/F_s(0)|$ (blue solid lines), experimental distribution of the supremum of the approximation $|F_s(u)/\mu_s(0)|$ (magenta solid lines), our estimation returned by (19) (red dashed lines), estimation (28) (orange solid lines) and estimation (29) (black solid lines). The values of ξ are in *dB*.

$F_{REF_2}(u)$ are very similar. This does not mean that the absolute difference between the reference and the thinned array factor is the same. Indeed, it results from the definition of the standardised error $\epsilon(u) = [F_s(u) - \mu_s(u)]/\sigma_s(u)$, which measures such a difference normalised to the standard deviation, and it is consistent with (14), which actually depends only on the threshold ξ. Second, it can be appreciated that (25) returns, as expected, values which are

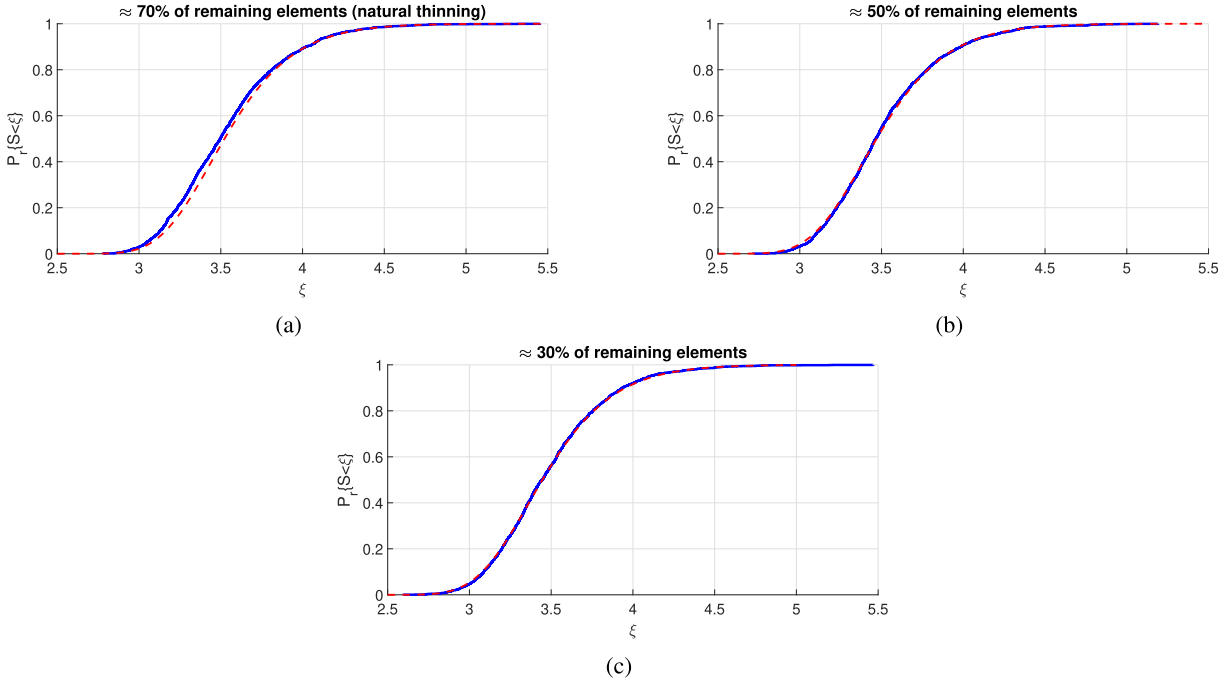

FIGURE 6. Probability distribution of $\mathcal{S}$ for $F_{REF_1}(u)$, $N = 1000$ and different levels of thinning: Experimental (blue solid lines), returned by (25) (red dashed lines). The values of ξ are in linear scale.

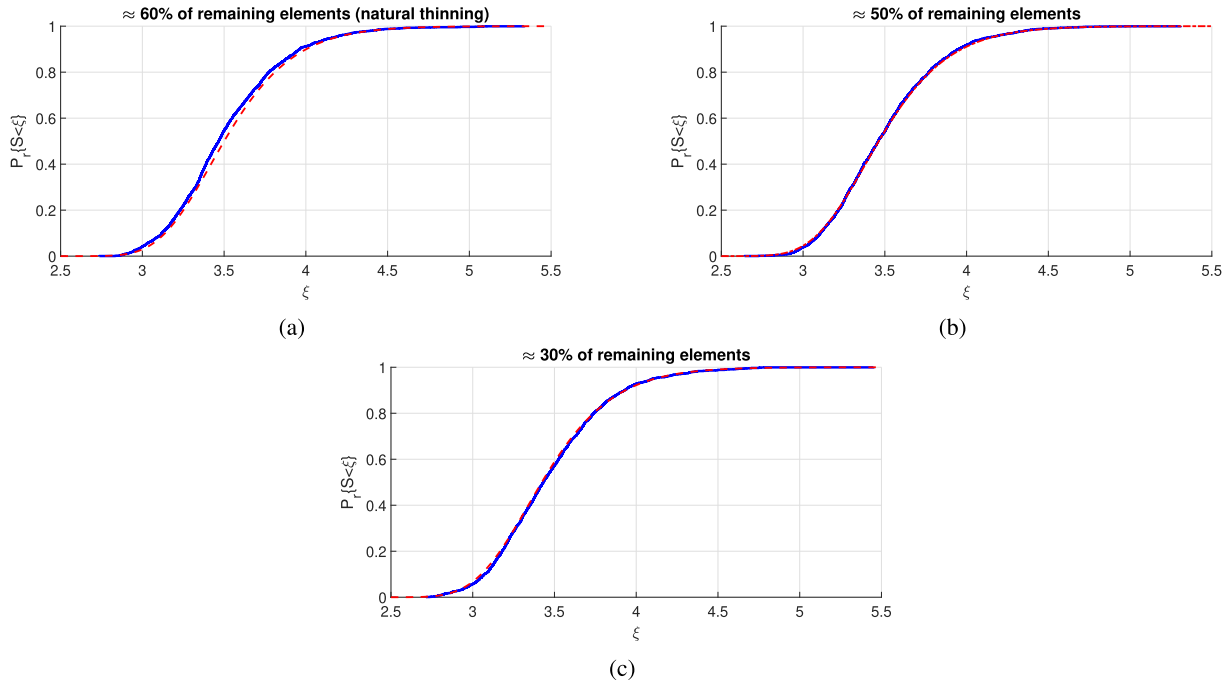

FIGURE 7. Probability distribution of $\mathcal{S}$ for $F_{REF_2}(u)$, $N = 1000$ and different levels of thinning: Experimental (blue solid lines), returned by (25) (red dashed lines). The values of ξ are in linear scale.

much smaller than the ones returned by the punctual characterisation given by (14). Indeed, for $\xi = 3$ the latter would return 99.73%. This emphasises the need for a global characterisation of the array factor. Finally, an analogous of (29) for estimating the probability distribution of $\mathcal{S}$ can be easily derived. However, as for the *PSLL*, it does not give results that are as good as the ones returned by (25).

As a concluding remark, we mention that the cases for $N = 200$ and $N = 100$ are omitted since the same circumstance

TABLE 1. Empirical statistics (in *dB*) of the *PSLL* for symmetric and asymmetric statistically thinned arrays with $N = 1000$ and for $\mu_s(u) = \mu(u) = F_{REF_1}(u)$ and $F_{REF_2}(u)$. The acronyms *r.e.*, *STAs* and *n.t.* stand for remaining elements, statistically thinned arrays and natural thinning, respectively.

		Symmetric $STAs$			Asymmetric $STAs$		
$\mu_s(u), \mu(u)$	$r.e.$	$min\{PSLL\}$	$mean\{PSLL\}$	$max\{PSLL\}$	$min\{PSLL\}$	$mean\{PSLL\}$	$max\{PSLL\}$
$F_{REF_1}(u)$	$\approx 70\%$ (n.t.)	-25.80	-22.72	-18.22	-27.66	-24.08	-20.07
	$\approx 50\%$	-22.14	-19.32	-15.75	-24.62	-22.23	-18.33
	$\approx 30\%$	-18.26	-15.56	-12.27	-21.63	-19.44	-15.57
$F_{REF_2}(u)$	$\approx 60\%$ (n.t.)	-25.34	-22.67	-19.29	-26.49	-24.71	-21.79
	$\approx 50\%$	-22.87	-20.25	-15.12	-24.02	-22.30	-19.07
	$\approx 30\%$	-18.40	-15.99	-12.50	-20.23	-17.94	-14.88

TABLE 2. Average relative side-lobe level (in *dB*) for symmetric (returned by (16)) and asymmetric (returned by (15)) statistically thinned arrays for $N = 1000$ and for $\mu_s(u) = \mu(u) = F_{REF_1}(u)$ and $F_{REF_2}(u)$. The acronyms *r.e.*, *STAs* and *n.t.* stand for remaining elements, statistically thinned arrays and natural thinning, respectively.

$\mu_s(u), \mu(u)$	$r.e.$	Symmetric $STAs$	Asymmetric $STAs$
$F_{REF_1}(u)$	$\approx 70\%$ (n.t.)	-31.80	-34.81
	$\approx 50\%$	-27.45	-30.45
	$\approx 30\%$	-23.52	-26.52
$F_{REF_2}(u)$	$\approx 60\%$ (n.t.)	-30.68	-33.69
	$\approx 50\%$	-28.18	-31.19
	$\approx 30\%$	-23.80	-26.80

TABLE 3. Empirical statistics (in linear scale) of δ when $N = 1000$ and for $\mu_s(u) = \mu(u) = F_{REF_1}(u)$ and $F_{REF_2}(u)$. The acronyms *r.e.* and *n.t.* stand for remaining elements and natural thinning, respectively.

$\mu_s(u), \mu(u)$	$r.e.$	$min\{\delta\}$	$mean\{\delta\}$	$max\{\delta\}$	$var\{\delta\}$
$F_{REF_1}(u)$	$\approx 70\%$ (n.t.)	0.89	1.27	1.80	0.02
	$\approx 50\%$	0.85	1.27	1.95	0.02
	$\approx 30\%$	0.88	1.26	1.87	0.02
$F_{REF_2}(u)$	$\approx 60\%$ (n.t.)	0.89	1.26	1.75	0.02
	$\approx 50\%$	0.87	1.27	1.85	0.02
	$\approx 30\%$	0.84	1.26	1.98	0.02

as for *PSLL* is obtained, *i.e.*, (25) still works very well in matching the experimental curves.

C. ASYMMETRIC VS SYMMETRIC THINNED ARRAYS

In this section we compare the assumed symmetric thinned array layout with the more general asymmetric case. This is done in order to appreciate how the *forced* symmetry impacts on the achievable performance. To this end, of course, the array aperture, the nominal number of radiators and the reference current are kept the same for both the symmetric and the asymmetric cases. Moreover, since $A_n = A_{-n} \ \forall \ n$, the desired (reference) array factor is the same for the two cases, *i.e.*, $\mu(u) = \mu_s(u)$.

As can be observed from Table 1, which compares the peak side-lobe level statistics, when the number of elements is high the deviation between the performance of the two types of array is not very significant, even though asymmetric arrays tend always to have slightly lower *PSLL*. In Table 2, the side-lobe level estimations returned by (15) and (16) is reported again for the two type of reference arrays considered above. It is seen that these commonly used estimations return strongly underestimated *PSLL*; once again highlighting the need for a more accurate *PSLL* prediction that we have tried to meet in this contribution.

Finally, the comparison in terms of the error between symmetric and asymmetric thinned arrays is also conducted by a Monte Carlo analysis, using the parameter

$$\delta = \frac{\max\{|F_s(u) - \mu_s(u)|\}}{\max\{|F(u) - \mu_s(u)|\}} \tag{30}$$

which represents the ratio between the maximum errors that the symmetric and the asymmetric thinned arrays present with respect to the desired array factor. The corresponding results are reported in Table 3. It can be observed that, in some cases $\delta < 1$, meaning that symmetric arrays performed better. As can be seen, on average, asymmetric thinned arrays perform slightly better than the symmetric ones. However, the *PSLL* and the standardised error results of symmetric arrays can be analytically foreseen and used as an upper bound for the former.

VI. CONCLUSION

We have shown that symmetric linear statistically thinned arrays and the asymmetric ones exhibit similar behaviours but the former have the advantage of being easier to characterise. In fact, we reported the analytical estimation of the probability distributions of the peak side-lobe level and of the supremum of the standardised error magnitude. Monte Carlo numerical experiments have shown that such estimations work very well so that they can be actually used to foresee, for

example, the peak side-lobe level according to the reference array factor and the degree of thinning.

We emphasise that, though this study was limited to the case of linear arrays, it can be directly applied, with minor modifications, to the case of planar/volumetric arrays when the latter are studied along the cuts of the radiation patterns. This is an important aspect that we intend to investigate in a future work.

Finally, we remark that our approach does not make certain assumptions that have been exploited in some previous literature results. For this reason, it proved to be much more precise than those results. Moreover, our approach is flexible and one can characterise the array factor not only on a generic portion of the full-scan range but also throughout the whole full-scan range, and, therefore, also taking into account the main-beam.

APPENDIX A

In this appendix we report the mathematical expressions of all the quantities that have not been explicitly given in the previous sections. The derivations are tedious but easy and hence are omitted. The aim is to give the reader all the details to implement our estimations.

In the asymmetric case, the variance of the real and imaginary parts of the array factor are

$$\sigma^2_{\mathcal{R}}(u) = \sum_{n=1}^{N} \frac{A_n}{\alpha} \left[\max\{A_n\} - \alpha A_n\right] \cos^2(2\pi x_n u) \tag{31}$$

and

$$\sigma^2_{\mathcal{I}}(u) = \sum_{n=1}^{N} \frac{A_n}{\alpha} \left[\max\{A_n\} - \alpha A_n\right] \sin^2(2\pi x_n u) \tag{32}$$

In the symmetric case, the mean and the variance of the derivative of the array factor, $F'_s(u) = dF_s(u)/du$, are

$$\mu_{F'}(u) = -4\pi \sum_{n=1}^{N/2} A_n x_n \sin(2\pi x_n u) \tag{33}$$

and

$$\sigma^2_{F'}(u) = 16\pi^2 \left\{ \sum_{n=1}^{N/2} x_n^2 \left[\frac{\max\{A_n\} A_n}{\alpha} - A_n^2 \right] \sin^2(2\pi x_n u) \right\} \tag{34}$$

The covariance between the array factor and its derivative is [20]

$$\begin{aligned} \mathcal{K}(u) &= \frac{1}{2} \frac{d\sigma_s^2(u)}{du} = \sigma_s(u)\, \sigma'_s(u) \\ &= -4\pi \sum_{n=1}^{N/2} x_n \left[\frac{\max\{A_n\} A_n}{\alpha} - A_n^2 \right] \sin(4\pi x_n u) \end{aligned} \tag{35}$$

with $\sigma'_s(u) = d\sigma_s(u)/du$ and the Bravais-Pearson correlation coefficient between $F_s(u)$ and $F'_s(u)$ is

$$\rho(u) = \frac{\mathcal{K}(u)}{\sigma_s(u)\sigma_{F'}(u)} \tag{36}$$

The mean of $\epsilon'(u)$ is zero for each u, whilst its variance is

$$\sigma^2_{\epsilon'}(u) = \frac{\sigma^2_{F'}(u) - \left\{\sigma'_s(u)\right\}^2}{\sigma^2_s(u)} \tag{37}$$

Finally, the covariance between $\epsilon(u)$ and its derivative is (taking into account that $\sigma^2_{\epsilon}(u) = 1$)

$$\mathcal{K}_{\epsilon\epsilon'}(u) = \frac{1}{2} \frac{d\sigma^2_{\epsilon}(u)}{du} = 0 \tag{38}$$

and so is the Bravais-Pearson correlation coefficient.

REFERENCES

[1] M. I. Skolnik, "Nonuniform arrays," in *Antenna Theory*, R. E. Collin and F. Zucker, Eds. New York, NY, USA: McGraw-Hill, 1969.
[2] O. M. Bucci, M. D'Urso, T. Isernia, P. Angeletti, and G. Toso, "Deterministic synthesis of uniform amplitude sparse arrays via new density taper techniques," *IEEE Trans. Antennas Propag.*, vol. 58, no. 6, pp. 1949–1958, Jun. 2010.
[3] R. M. Leahy and B. D. Jeffs, "On the design of maximally sparse beamforming arrays," *IEEE Trans. Antennas Propag.*, vol. 39, no. 8, pp. 1178–1187, Aug. 1991.
[4] H. Unz, "Linear arrays with arbitrarily distributed elements," *IRE Trans. Antennas Propag.*, vol. 8, no. 2, pp. 222–223, Mar. 1960.
[5] R. E. Willey, "Space tapering of linear and planar arrays," *IRE Trans. Antennas Propag.*, vol. 10, no. 4, pp. 369–377, Jul. 1962.
[6] M. Andreasen, "Linear arrays with variable interelement spacings," *IRE Trans. Antennas Propag.*, vol. 10, no. 2, pp. 137–143, Mar. 1962.
[7] R. F. Harrington, "Sidelobe reduction by nonuniform element spacing," *IRE Trans. Antennas Propag.*, vol. 9, no. 2, pp. 187–192, Mar. 1961.
[8] O. M. Bucci and S. Perna, "A deterministic two dimensional density taper approach for fast design of uniform amplitude pencil beams arrays," *IEEE Trans. Antennas Propag.*, vol. 59, no. 8, pp. 2852–2861, Aug. 2011.
[9] A. Ishimaru, "Theory of unequally-spaced arrays," *IRE Trans. Antennas Propag.*, vol. 10, no. 6, pp. 691–702, 1962.
[10] A. Ishimaru and Y.-S. Chen, "Thinning and broadbanding antenna arrays by unequal spacings," *IEEE Trans. Antennas Propag.*, vol. AP-13, no. 1, pp. 34–42, Jan. 1965.
[11] A. Ishimaru, "Unequally spaced arrays based on the Poisson sum formula," *IEEE Trans. Antennas Propag.*, vol. 62, no. 4, pp. 1549–1554, Apr. 2014.
[12] M. I. Skolnik, J. Sherman, III, and F. Ogg, Jr., "Statistically designed density-tapered arrays," *IEEE Trans. Antennas Propag.*, vol. AP-12, no. 4, pp. 408–417, Jul. 1964.
[13] Y. T. Lo, "Random periodic arrays," *Radio Sci.*, vol. 3, no. 5, pp. 425–436, May 1968.
[14] Y. T. Lo, "A mathematical theory of antenna arrays with randomly spaced elements," *IEEE Trans. Antennas Propag.*, vol. AP-12, no. 3, pp. 257–268, May 1964.
[15] R. L. Haupt, *Antenna Arrays: A Computational Approach*. Hoboken, NJ, USA: Wiley, 2010.
[16] R. J. Mailloux, *Phased Array Antenna Handbook*, 2nd ed. Norwood, MA, USA: Artech House, 2005.
[17] P. Rocca and R. L. Haupt, "Dynamic array thinning for adaptive interference cancellation," in *Proc. 4th Eur. Conf. Antennas Propag. (EuCAP)*, 2010, pp. 1–3.
[18] R. L. Haupt, "Adaptively thinned arrays," *IEEE Trans. Antennas Propag.*, vol. 63, no. 4, pp. 1626–1632, Apr. 2015.
[19] B. D. Steinberg, "The peak sidelobe of the phased array having randomly located elements," *IEEE Trans. Antennas Propag.*, vol. AP-20, no. 2, pp. 129–136, Mar. 1972.
[20] G. Buonanno and R. Solimene, "Large linear random symmetric arrays," *Prog. Electromagn. Res. M*, vol. 52, pp. 67–77, Nov. 2016.
[21] V. D. Agrawal and Y. T. Lo, "Distribution of sidelobe level in random arrays," *Proc. IEEE*, vol. 57, no. 10, pp. 1764–1765, Oct. 1969.
[22] M. Donvito and S. A. Kassam, "Characterization of the random array peak sidelobe," *IEEE Trans. Antennas Propag.*, vol. AP-27, no. 3, pp. 379–385, May 1979.

[23] S. Krishnamurthy, D. W. Bliss, and V. Tarokh, "Sidelobe level distribution computation for antenna arrays with arbitrary element distributions," in *Proc. Conf. Rec. 45th Asilomar Conf. Signals, Syst. Comput. (ASILOMAR)*, Pacific Grove, CA, USA, Nov. 2011, pp. 6–9.
[24] C. A. Balanis, *Antenna Theory: Analysis and Design*, 2nd ed. New York, NY, USA: Wiley, 1996.
[25] N. Fourikis, *Advanced Array Systems, Applications and RF Technologies* (Signal Processing and its Applications). 1st ed. New York, NY, USA: Academic, 2000.
[26] M. Zelen and N. C. Severo, "Probability functions," in *Handbook of Mathematical Functions With Formulas, Graphs and Mathematical Tables*, M. Abramowitz and I. A. Stegun, Eds. Washington, DC, USA: Government Printing Office, Dec. 1972.
[27] L. W. Couch, *Digital and Analog Communication Systems*, 6th ed. Upper Saddle River, NJ, USA: Prentice-Hall, 2001.
[28] G. Buonanno and R. Solimene, "Generalised random binned antenna arrays," *Prog. Electromagn. Res. C*, vol. 78, pp. 129–143, Oct. 2017.
[29] G. Buonanno and R. Solimene, "Unequally excited generalised random binned antenna arrays," *IET Microw., Antennas Propag.*, vol. 13, no. 14, pp. 2531–2538, Nov. 2019.
[30] G. Buonanno and R. Solimene, "Unequally-excited linear totally random antenna arrays for multi-beam patterns," *IET Microw., Antennas Propag.*, vol. 12, no. 10, pp. 1671–1678, Aug. 2018.
[31] G. Buonanno and R. Solimene, "Study of unequally-excited random antenna arrays for beam shaping," *Prog. Electromagn. Res. C*, vol. 85, pp. 129–140, Jul. 2018.
[32] G. Buonanno and R. Solimine, "Probabilistic density-tapered antenna arrays," in *Proc. Prog. Electromagn. Res. Symp. (PIERS-Toyama)*, Toyama, Japan, Aug. 2018, pp. 1–4.
[33] G. Buonanno and R. Solimene, "Phase-only excited random antenna arrays," in *Proc. Prog. Electromagn. Res. Symp. (PIERS-Toyama)*, Toyama, Japan, Aug. 2018, pp. 1–4.
[34] S. O. Rice, "Mathematical analysis of random noise," *Bell Syst. Tech. J.*, vol. 23, pp. 282–332, Jul. 1944.
[35] H. Cramér and M. R. Leadbetter, *Stationary and Related Stochastic Processes: Sample Function Properties and Their Applications*. New York, NY, USA: Dover, 2004.
[36] W. Feller, *An Introduction to Probability Theory and its Applications*, vol. 2. New York, NY, USA: Wiley, 1966.
[37] T. T. Taylor, "Design of line-source antennas for narrow beamwidth and low side lobes," *Trans. IRE Prof. Group Antennas Propag.*, vol. 3, no. 1, pp. 16–28, Jan. 1955.

GIOVANNI BUONANNO received the M.S. degree *summa cum laude* in electronic engineering from the Seconda Università degli Studi di Napoli (SUN), Aversa, Italy, in 2014. Then, he joined the Research Group in applied electromagnetics with SUN. In 2015, he began his Ph.D. program in industrial and information engineering, completing it with the University of Campania Luigi Vanvitelli, in 2018, where he is currently a Research Fellow. His main research interests include the analysis and design of nonuniformly spaced antenna arrays and microwave imaging.

RAFFAELE SOLIMENE (Senior Member, IEEE) received the Laurea *summa cum laude* and the Ph.D. degrees in electronic engineering from the Seconda Università degli Studi di Napoli (SUN), Aversa, Italy, in 1999 and 2003, respectively. In 2002, he became an Assistant Professor with the Faculty of Engineering, Mediterranea University of Reggio Calabria, Italy. Since 2006, he has been with the Dipartimento di Ingegneria, University of Campania Luigi Vanvitelli, where he is currently an Associate Professor. Based on the following topics, he has coauthored more than 250 scientific works. His research interests include inverse electromagnetic problems with applications to inverse source and array diagnostics, non-destructive subsurface investigations, through-the-wall and GPR imaging, and breast cancer detection. On these topics, he routinely serves as a Reviewer for a number of journals and organized several scientific sessions. He is also an Associate Editor for four scientific journals, among which IEEE Geoscience and Remote Sensing Letters.